COBEM 2023 27TH INTERNATIONAL CONGRESS OF MECHANICAL ENGINEERING

ABCM Brazilian Society of Mechanical Sciences and Engineering
27th ABCM International Congress of Mechanical Engineering
December 04-08, 2023, Florianópolis-SC, Brazil

COB-2023-1214
NUMERICAL MODELLING AND SIMULATION OF MEMBRANES FOR SEPARATING GASES IN SUPERCRITICAL STATE

Flávio Silva Ferro
Bruno Souza Carmo
Department of Mechanical Engineering, Escola Politécnica, University of São Paulo
Av. Professor Mello Moraes, 2231
flavioferro@usp.br
bruno.carmo@usp.br

Abstract. *The utilization of membranes for gas separation processes has gained momentum due to its numerous advantages. This article focuses on the separation of gases, with a particular emphasis on the critical CO_2 and CH_4 separation. Membrane-based separation offers cost-effective solutions and easy scalability compared to other technologies. This research delves into the relatively unexplored domain of using membranes for gas separation in supercritical conditions. The study investigates the influence of geometric parameters on membrane modules using Computational Fluid Dynamics (CFD) modeling and simulations, employing the finite element method in the commercial software COMSOL. The Soave-Redlich-Kwong real gas model was used within the software. The findings suggest that temperature plays a crucial role in expediting the process. However, in supercritical conditions, the separation efficiency might be compromised. Surprisingly, many of the geometric parameters were found to have limited relevance. These findings contribute to a deeper understanding of membrane-based gas separation in supercritical conditions and shed light on the significance of various parameters involved in the process.*

Keywords: *membranes, gas separation, supercritical conditions, CFD, COMSOL, real model gas*

1. INTRODUCTION

A crucial step in the handling of feedstock gas is the removal of acid gases such as CO_2 and SO_2 before pressurized, stored or transported. The separation of the CO_2 from the CH_4 in natural gas and biogas streams is extremely important since high concentrations of CO_2 can imply direct release of this component in nature, unwanted contamination in chemical processes, and decrease of net calorific value if the gas is used as fuel. The pressurizing of oil wells using CO_2 for enhanced oil recovery and, consequently, its storage in these places is an extremely interesting solution in relation to the emission of greenhouse gases (Figueroa *et al.*, 2008; Lin and Freeman, 2004).

A simple process technology that can be applied in remote, unattended, or offshore situations is highly desirable. Ease of operation, quick start-up, and high on-stream factors are needed in addition to competitive capital and operating costs. Traditional methods for CO_2 capture are based on reversible absorption, such as amine scrubbing, but these processes are energy intensive and pose environmental concerns. The advantages of membrane gas separation over traditional techniques like chemical absorption by reactive solvents and cryogenic separation include low-energy consumption, ease of operation, and low environmental impact. However, the separation of the CO_2 by membranes of selective permeability is a technology still in development, and the flux and the selectivity of current commercial polymeric membranes are too low to process large volumes of gas (Yang *et al.*, 2008).

The membrane separation process may be classified, for example, by the flow regime, mechanism, mode of operation and membrane constituent material, high pressure or low pressure processes in configurations known as cross flow or dead-end. In relation to their porosity, we can classify them as porous and non-porous; as symmetrical and asymmetrical in relation to their structure; organic and inorganic materials given the constitution material. Depending on the type of membrane or the filter module assembly, the arrangement of the passage ducts of the fluid can result in an unnecessary loss of pressure that can be avoided with a re-evaluation of the design (Gu, 2022).

Many studies have been developed to simulate and optimize the use of membranes for gas separation. Usually, the membranes are modelled like hollow fibers or infinite plates and their separation process is improved with spacers and orifices that promote better mixing of the feed stream, which also changes the membrane's properties (Alkhamis *et al.*, 2015a,b; Alrehili *et al.*, 2016; Qadir *et al.*, 2019). Other membrane technologies were also studied, like the use of modified silicon carbide nanosheets (Bayat *et al.*, 2020), and yet, there are a few works which focus on the simulations in large scale and in membrane modules (Bayat *et al.*, 2020; Gu, 2022). Thus, there is a lack of research focused on the membrane gas separation process in supercritical states and just a few concerned with the geometric arrangement of the membranes with the purpose of optimizing the separation modules.

This work aims to fill this information gap by simulating the gas separation process in supercritical states and exploring various geometric conditions to assess their influence. These simulations employ the finite element method and a real gas model, ensuring more reliable results. A better understanding of the gas separation process can lead to cost savings and increased efficiency, making it more affordable. Moreover, an improved gas separation process can enhance access to clean energy sources by capturing and utilizing valuable gases, while also reducing harmful emissions to mitigate climate change.

2. MATHEMATICAL MODELLING

One notable aspect of this research is the utilization of a real gas model to study the gas separation process with membranes. The thermodynamic Soave-Redlich-Kwong model, implemented in COMSOL, was employed for this purpose. In terms of the flow characteristics, laminar flow was considered, governed by the Navier-Stokes equations, and the species transport in the membrane was governed by Fick's diffusion law.

The separation process is given by a difference pressure between the feed and permeate sides, resulting in a flux of the species to the permeate. The flux, also depends on the permeance of which gas in it, principal in charge of the separation.

Regarding the geometry, initial analyses were performed using an axisymmetric model. However, further investigations also explored 3D models. The gas separation process with membranes can be implemented in different configurations, such as shell-side feed and bore-side feed. Additionally, the flow direction can be adjusted, resulting in co-current flow or countercurrent flow configurations. However, almost all the simulations shown here are done with the shell-side feed and co-current flow configuration. A schematic representation of this model can be seen in Figure 1.

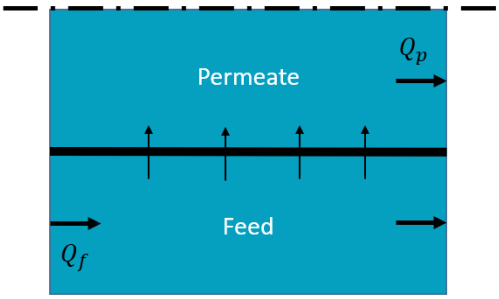

Figure 1: Schematic representation of the model

2.1 Soave-Redlich-Kwong real model gas

The Soave-Redlich-Kwong real model gas enables the calculation of gas properties under the specific temperature and pressure conditions required for the other physics involved in the problem, and its equation of state is given by

$$P = \frac{RT}{V-b} - \frac{a\alpha}{V(V+b)} \tag{1}$$

$$\alpha = \frac{1}{\sqrt{T}} \tag{2}$$

where P is the pressure, R is the gas constant, T is the temperature, V is the volume and as we have a mixture, a and b are calculated with the expressions

$$a = \sum_i \sum_j x_i x_j (-K_{SRK,i,j}) \sqrt{a_i a_j} \tag{3}$$

$$b = \sum_i x_i b_i \tag{4}$$

$$a_i = \frac{\Omega_A R^2 T^{2.5}}{P_c} \tag{5}$$

$$b_i = \frac{\Omega_B R T_c}{P_c} \tag{6}$$

$$\Omega_A = \frac{1}{3} + \frac{1}{3}\Omega_B(3 + 3\Omega_B) \tag{7}$$

$$\Omega_B = \frac{1}{27} 2^{\frac{1}{3}} 27^{\frac{2}{3}} - \frac{1}{3} \tag{8}$$

with x_i being the molar fraction of species i, $k_{SRK,i,j}$ being a tabulated value and the subscript c refers to the critical temperature and pressure (COMSOL, 2018).

2.2 Laminar flow

The laminar flow was modelled based on the Navier-Stokes equations, considering a compressible flow with Mach less than 0.3, meaning that viscosity and density variations with temperature are being considered. The continuity equation and the momentum equation for a single-phase fluid are, respectively,

$$\frac{\partial \rho}{\partial t} + \nabla \cdot (\rho \mathbf{u}) = 0, \tag{9}$$

$$\rho \frac{\partial \mathbf{u}}{\partial t} + \rho \mathbf{u} \cdot \nabla \mathbf{u} = -\nabla p + \nabla \cdot (\mu(\nabla \mathbf{u} + (\nabla \mathbf{u})^T) - \frac{2}{3}\mu(\nabla \cdot \mathbf{u})I) + \mathbf{F}. \tag{10}$$

In these equations, ρ is the density, $\mathbf{u}$ the velocity vector, p is pressure, μ is the dynamic viscosity and $\mathbf{F}$ is the volume force vector (COMSOL, 2018).

For the walls, we considered slip and no slip conditions, depending on the wall. The no slip condition assumes that there are viscous effects at the wall, so the relative velocity of the fluid particle in contact with the wall is zero, and hence, boundary layers can develop. Since we are dealing with stationary no slip walls, the boundary condition we employ is given by $\mathbf{u} = 0$. For the slip condition, we consider that there is no flow across the boundary and nor viscous stress in the tangential direction (COMSOL, 2018). This condition is described by

$$\mathbf{u} \cdot \mathbf{n} = 0, \tag{11}$$

$$\mathbf{K} - (\mathbf{K} \cdot \mathbf{n})n = 0, \tag{12}$$

$$\mathbf{K} = \mu(\nabla \mathbf{u} + (\nabla \mathbf{u})^T \mathbf{n}, \tag{13}$$

where $\mathbf{n}$ is the unit vector normal to the wall.

2.3 Transport of species

We used the Transport of Diluted Species environment for modelling the transport by diffusion and convection of the species. The mass balance equation for a species i is

$$\frac{\partial c_i}{\partial t} + \nabla \cdot \mathbf{J}_i + \mathbf{u} \cdot \nabla c_i = R_i, \tag{14}$$

$$\mathbf{J}_i = D_i \nabla c_i, \tag{15}$$

where c_i is the concentration of the species, D_i denotes the diffusion coefficient, R_i is the reaction rate expression, and $\mathbf{J_i}$ the mass flux diffusive flux vector (COMSOL, 2019). The diffusion coefficients were calculated by the Champman-Enskog Theory,

$$D_{i,j} = \frac{1.86 \cdot 10^{-3} T^{3/2} (1/M_i + 1/M_j)^{1/2}}{p \sigma_{i,j}^2 \omega}, \tag{16}$$

in which $D_{i,j}$ is in cm^2/s, p is the pressure in atmospheres and M_i are the molecular weights, $\sigma_{i,j}$ is the collision diameter, given in angstroms and is the arithmetic average of the two species, and ω is the integration of the interaction, described by the Lennard-Jones potential between the species (Cussler, 2009).

For the transport through the membrane, the permeance and the partial pressures were considered and the flux was calculated by

$$\mathbf{J}_i \cdot \mathbf{n} = P_i(p_{i,f} - p_{i,p}), \tag{17}$$

$$p_i = x_i p, \tag{18}$$

$$x_i = \frac{c_i}{\sum_{j=i}^{n} c_j}, \tag{19}$$

where P_i is the permeance of the species i and p_i is the partial pressure (in the feed and in the permeate) (Cussler, 2009).

We considered that the permeance varied with the temperature and was calculated with the Arrhenius equation,

$$P_i = A_i e^{(-\frac{E_{act,i}}{RT})}, \tag{20}$$

where A_i is a constant and E_{act} is the activation energy. The activation energy and the constants A_i were found linearizing the equation and fitting a line equation with know experimental values taken from (Tranchino *et al.*, 1989) and Duan *et al.* (2023).

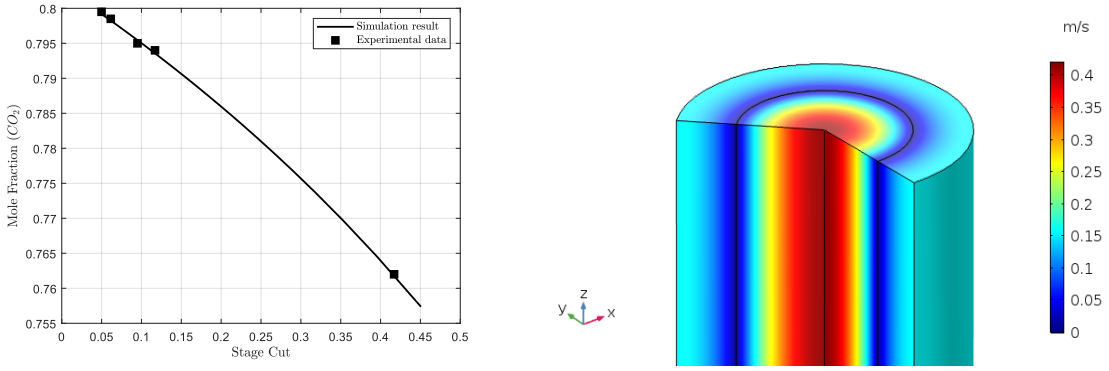

(a) (b)

Figure 2: (a) Model validation; (b) Velocity field

2.4 Uncertainty quantification – Monte Carlo method

Uncertainty quantification (UQ) is a crucial discipline that aims to assess and manage uncertainties in mathematical models, simulations, and data analysis. Among the many techniques available, the Monte Carlo method stands out as a powerful and widely used approach for uncertainty quantification (McClarren, 2018).

The Monte Carlo method is a statistical sampling technique used to estimate complex systems' behaviors by generating multiple random samples. The input parameters of the mathematical model were defined, along with their respective probability distributions. For each sample, the model was evaluated, producing an output variable of interest (McClarren, 2018). The method allows to fit a probability distribution of a variable of interest and other statistical measures.

The important input parameters T, $x_{(co_2,inlet)}$, $\alpha_{\text{permeance}}$ and β_{pressure} were chosen, no more parameters were picked up because of the significant growth of number of samples necessary to the UQ. The $\alpha_{\text{permeance}}$ and β_{pressure} were defined, respectively, by

$$\alpha_{\text{permeance}} = \frac{P_{\text{CO}_2}}{P_{\text{CH}_4}} \tag{21}$$

and

$$\beta_{\text{pressure}} = \frac{p_{\text{feed}}}{p_{\text{permeate}}}. \tag{22}$$

3. VALIDATION

The developed model was validated with experimental data from the bibliography for an experiment of CO_2/CH4 separation (Tranchino *et al.*, 1989). In Figure 2 we show a plot of the molar fraction of CO_2 in the permeate by the stage cut and, in Table 1, we present the values we used for some parameters of the simulations. These values were obtained from Tranchino *et al.* (1989) and Gilassi *et al.* (2017).

In the analyses below, we refer to the stage cut (θ), which is a fraction of how much of the flow of the feed (Q_f) goes to the permeate (Q_p),

$$\theta = \frac{Q_p}{Q_f}. \tag{23}$$

After the validation, we proceed to the uncertainty quantification, employing the Monte-Carlo method with thirty thousand simulations. The input parameters defined and their variance are given in Table 2. We have considered a normal distribution for all of them.

We got an average of 0.78 with a standard deviation of 0.05, so it was considered that the numerical model has a standard deviation of 6.41% in relation to the results. With this information, we plotted the Normal fit with the data histogram, as well the convergence of the average, in Figure 3.

4. RESULTS AND DISCUSSION

First, the real gas model based on the Soave-Redlich-Kwong theory was introduced. The focus of the study was on analyzing the CO_2 mole fraction in the permeate at the end of the process under supercritical conditions. Temperature and

Table 1: Parameters of the simulation

Parameter	**Unit**	**Value**
Fiber Radius	μm	195
Shell Width	μm	133
Length	cm	15
Temperature	K	298
Feed Pressure	kPa	400
Permeate Pressure	kPa	100
Permeance	$\mathrm{mol\,s^{-1}\,m^{-2}\,Pa^{-1}}$	$1.072 \cdot 10^{-10}$ CO_2
		$2.989 \cdot 10^{-10}$ CH_4
Feed Composition		60% CO_2
		40% CH_4

Table 2: Parameters and its variances

Parameter	**Variance**
T	2
$x_{\mathrm{CO_2,inlet}}$	0.005
$\alpha_{\mathrm{permeance}}$	0.51
$\beta_{\mathrm{pressure}}$	0.28

pressure were varied, the temperature ranged from 300 to 500 K and the pressure from 7.5 to 10 MPa, motivating the use of a real gas model. The permeance model given by the Arrhenius equation was used. We performed a sweep in pressure values imposed in the feed, and the difference pressure between the feed and the permeate (300 kPa) was maintained.

In the simulation, a mesh with a total of $3,750$ elements was employed to discretize the domain and capture the flow behavior. The simulation assumed a steady-state condition. The boundary conditions were as follows. At the inlet boundary, a fixed flow was imposed, while at the outlet boundary a pressure outlet condition was applied. Additionally, slip or no-slip conditions were applied at the walls, depending on the case. For mass transport, the concentration of the species was also imposed at the inlet boundary. At the membrane wall, the flux from the feed to the permeate was defined using Eq. (17). The obtained results were visualized through a surface plot, which is shown in Figure 4.

As can be observed, the gas separation process did not achieve high efficiency, despite having a feed stream with 60% of CO_2. Another important aspect investigated was the influence of temperature and pressure on the stage cut. A surface plot depicting this relationship is presented in Figure 5. It can be seen that the temperature has a significant impact on the stage cut, whereas pressure does not show a notable influence. This suggests that manipulating the temperature could potentially enhance the efficiency of the gas separation process, allowing for shorter membrane modules to achieve the desired outcome. However, the associated costs should be carefully considered.

Next, 3D models were employed to analyze the packing factors and bundle arrangement, using the same parameters as in the validation study. In this analysis, a parameter called γ, representing the ratio between the distance from the center

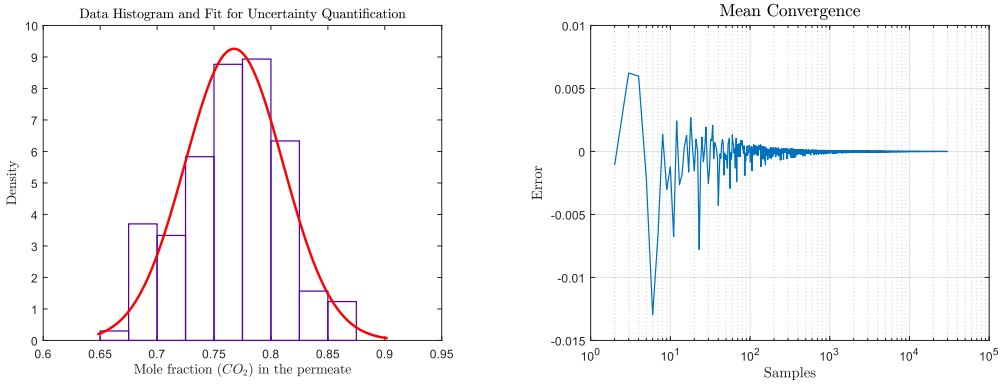

(a) (b)

Figure 3: (a) Normal fit; (b) Convergence of UQ

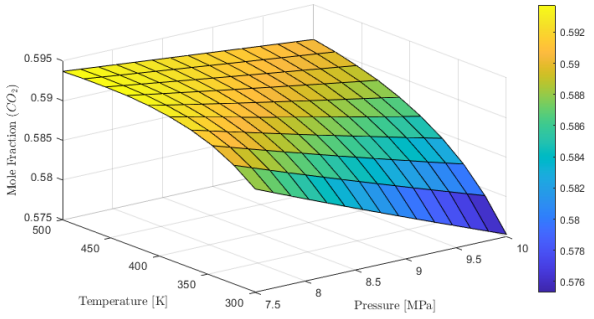

Figure 4: Mole fraction of CO_2 at the end of permeate varying pressure and temperature

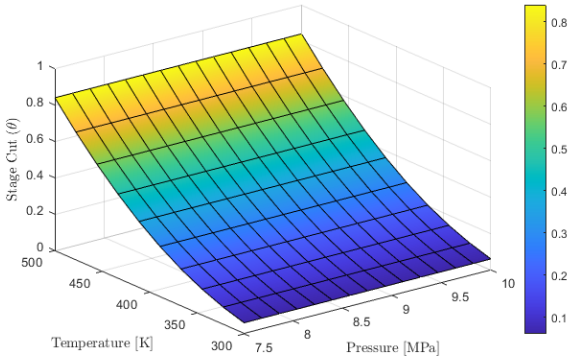

Figure 5: Influence of pressure and temperature on stage cut

to one of the edges of the polygon and the radius of the fiber, was introduced,

$$\gamma = \frac{d}{r}. \tag{24}$$

This parameter serves as a measure of the packing factor, allowing us to assess its influence on the gas separation process. An example of the hexagonal arrangement is presented in Figure 6.

For the 3D simulations, the meshes consisted of more than $300,000$ elements, and a steady-state condition was also considered. The boundary conditions for the 3D simulations were the same as those in the axisymmetric case, with the addition of a periodic condition at the opposite pairs of walls for each polygon. On these walls, the concentration of species, velocity, and pressure are imposed to be equal, to account for the presence of other membranes with the same properties surrounding the one under study.

We studied the quadrangular, hexagonal and octagonal geometric packing, with the same γ. The results show that there is not a large difference between the geometric packings and varying γ did not change much the results as we can see in Figure 7.

Additionally, the pressure drop across the feed was investigated while varying the γ parameter. The pressure drops are presented in Table 3, revealing significant differences between the different configurations. It is important to note that a higher pressure drop corresponds to a greater energy requirement for operating the process. Therefore, choosing the configuration with the lower pressure drop may be more favorable. Since the efficiency of the gas separation process

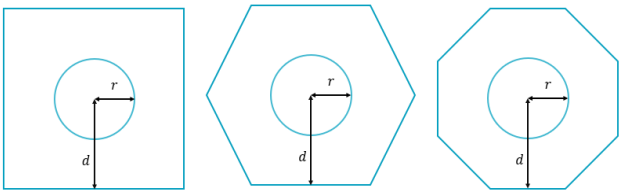

Figure 6: Geometric arrangements (the opposing edges of the geometries had periodic boundary conditions).

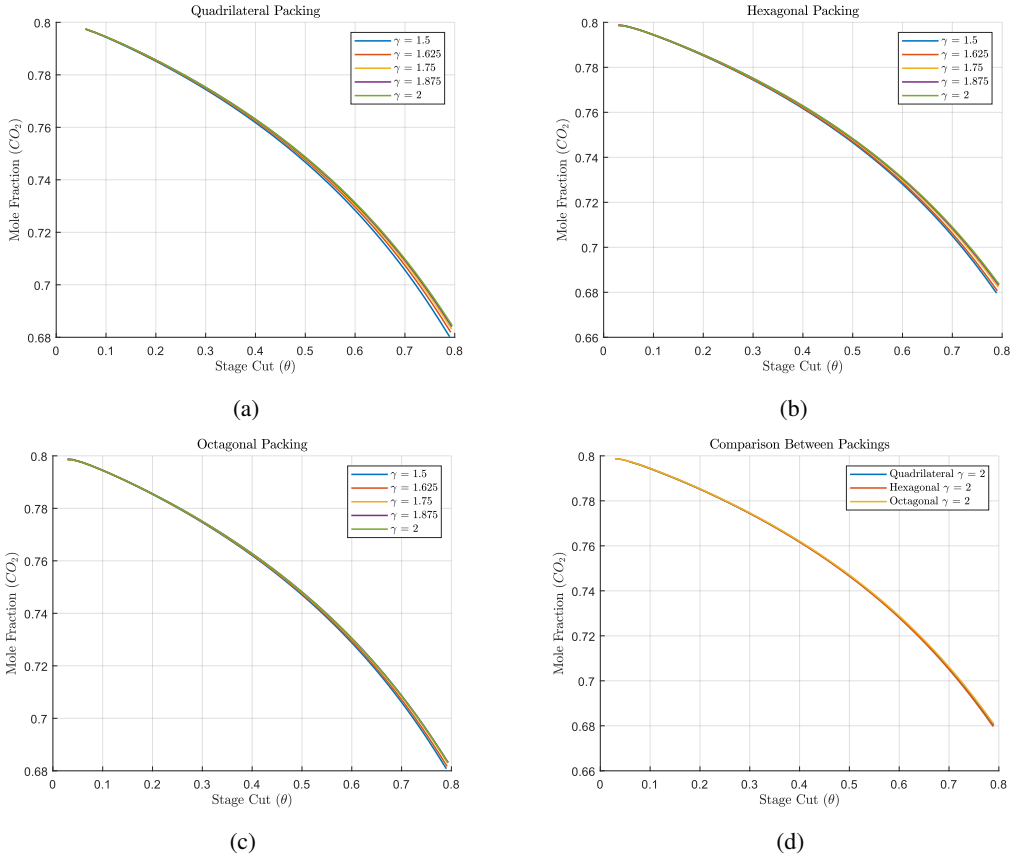

Figure 7: (a) Separation in quadrangular packing; (b) Separation in hexagonal packing; (c) Separation in octagonal packing; (d) Comparison between arrangements with $\gamma = 2$

Table 3: Total pressure drop in each arrangement and γ

γ	ΔP **Quadrilateral [Pa]**	ΔP **Hexagonal [Pa]**	ΔP **Octagonal [Pa]**
1.5	24.55	48.00	58.97
1.625	13.24	24.46	29.29
1.75	7.71	13.65	16.28
1.875	4.79	8.22	9.69
2	3.16	5.26	6.18

does not show substantial differences among the configurations, it is possible to achieve comparable efficiency with lower energy costs.

5. CONCLUSION

In conclusion, this study investigated the gas separation process using membranes and explored various factors that can influence its efficiency. The implementation of a real gas model, specifically the Soave-Redlich-Kwong theory, provided valuable insights into the behavior of gases under supercritical conditions. The analysis of CO_2 mole fraction in the permeate revealed that the separation efficiency was not optimal, indicating room for improvement. Additionally, the study examined the impact of temperature and pressure on the process, highlighting the significant influence of temperature on the stage cut. These findings suggest that temperature control can potentially enhance the efficiency of gas separation, potentially reducing the length of membrane modules while maintaining desired results. However, the cost implications must also be considered. Furthermore, the investigation of different packing factors and bundle arrangements in a 3D model demonstrated the importance of optimizing the packing factor to improve the gas separation process. The pressure drop analysis indicated that configurations with lower pressure drop requirements may be more energy-efficient, offering potential cost savings during operation. Overall, this study contributes to a better understanding of the gas separation process using membranes. These insights can inform the design and optimization of membrane-based gas separation

systems, ultimately enabling more efficient and cost-effective industrial applications.

6. REFERENCES

Alkhamis, N., Anqi, A.E. and Oztekin, A., 2015a. "Computational study of gas separation using a hollow fiber membrane". *International Journal of Heat and Mass Transfer*, pp. 749–759.

Alkhamis, N., Oztekin, D.E., Alsaiari, A. and Oztekin, A., 2015b. "Numerical study of gas separation using a membrane". *International Journal of Heat and Mass Transfer*, pp. 835–843.

Alrehili, M., Usta, M., Alkhamis, N., Anqi, A.E. and Oztekin, A., 2016. "Flows past arrays of hollow fiber membranes – gas separation". *International Journal of Heat and Mass Transfer*, pp. 400–411.

Bayat, G., Saghatchi, R., Azamat, J. and Khataee, A., 2020. "Separation of methane from different gas mixtures using modified silicon carbide nanosheet: Micro and macro scale numerical studies". *Chinese Journal of Chemical Engineering*, pp. 1268–1276.

COMSOL, 2018. "Chemical reaction engineering module". COMSOL Multiphysics.

COMSOL, 2019. "Comsol multiphysics reference manual". COMSOL Multiphysics.

Cussler, E.L., 2009. *Diffusion Mass Transfer in Fluid Systems*. Cambridge University Press.

Duan, S., Li, D., Yang, X., Niu, C., Sun, S., He, X., Shan, M. and Zhang, Y., 2023. "Experimental and molecular simulation study of a novel benzimidazole-linked polymer membrane for efficient h2/co2 separation". *Journal of Membrane Science*, pp. 1–9.

Figueroa, J., Fout, T., Plasynski, S., Mcilvried, H. and Srivastava, R., 2008. "Advances in co2 capture technology". *International Journal of Greenhouse Gas Control*, pp. 9–20.

Gilassi, S., Taghavi, M.S., Rodrigues, D. and Kaliaguine, S., 2017. "Simulation of gas separation using partial element stage cut modeling of hollow fiber membrane modules". *AIChE Journal*, pp. 1–12.

Gu, B., 2022. "Mathematical modelling and simulation of co2 removal from natural gas using hollow fibre membrane modules". *Korean Chem. Eng. Res.*, pp. 51–61.

Lin, H. and Freeman, B., 2004. "Gas solubility, diffusivity and permeability in poly (ethylene oxide)". *Journal of Membrane Science*, pp. 105–117.

McClarren, R.G., 2018. *Uncertainty Quantification and Predictive Computational Science*. Springer.

Qadir, S., Hussain, A. and Ahsan, M., 2019. "A computational fluid dynamics approach for the modeling of gas separation in membrane modules". *Processes*, pp. 1–13.

Tranchino, L., Santarossa, F., Carta, F., Fabiani, C. and Bimbi, L., 1989. "Gas separation in a membrane unit: Experimental results and theorical predictions". *Separation Science and Technology*, pp. 1207–1226.

Yang, H., Xu, Z., Fan, M., Gupta, R., Slimane, R., Bland, A. and Wright, L., 2008. "Progress in carbon dioxide separation and capture: a review". *Journal of Environmental Sciences*, pp. 14–27.

7. RESPONSIBILITY NOTICE

The authors are the only responsible for the printed material included in this paper.